Article

Investigation of Luliconazole-Loaded Mucoadhesive Electrospun Nanofibers for Anticandidal Activity in the Management of Vaginal Candidiasis

Arya Vidyadhari, Nidhi Singh, Avinash Kumar Singh, Tanya Ralli, Pratima Solanki, M Aamir Mirza, Suhel Parvez,* and Kanchan Kohli*

Read Online

ACCESS | Metrics & More | Article Recommendations

ABSTRACT: In this study, we fabricated and evaluated luliconazole-loaded electrospun nanofibers for anticandidal activity in the management of vaginal candidiasis. Polycaprolactone (PCL)/gelatin nanofibers were designed by the electrospinning technique, and the Box–Behnken design (BBD) was adopted for optimization to get tailored fibers. The luliconazole (LCZ) drug was mixed into different concentrations (2.5, 5, 7.5, and 10%) of tea tree oil (TT oil) and loaded into the PCL/gelatin nanofibrous mats. The effective anticandidal potential of nanofiber samples were analyzed by the disk-diffusion method. Scanning electron microscopy (SEM), Fourier transform infrared (FTIR), differential scanning calorimetry (DSC), XRD analysis, and in silico study were performed. The entrapment efficiency, swelling degree, mechanical strength, contact angle, mucoadhesion, drug release, and permeation study were assessed. The average diameter of the PCL/gelatin-optimized nanofiber was 153 nm. SEM reflected that the fabricated nanofibers were uniform and bead-free. FTIR and DSC analyzed the interaction and physical entrapment of the drug in the polymeric fibers. The entrapment efficiency of the drug-loaded nanofiber was found to be 89.2 ± 0.8%. Maximum swelling percentages at 4 h were 40.8, 18.9, and 14.0% and contact angles were 46.5°, 62.95°, and 65.78° for the blank, TT oil-loaded, and drug-loaded nanofiber, respectively, which indicated the hydrophilic nature of the fibers. The drug-loaded nanofiber had a high tensile strength with satisfactory mucoadhesive property that led to its adhesion to the vaginal mucosa with no tear. The drug-loaded nanofiber had a cumulative drug release of 67.7 ± 3.4% in 48 h, and the 12.8 ± 0.53 mm of zone of inhibition (ZOI) in 48 h illustrated an effective anticandidal activity. The TT oil-loaded nanofiber also exhibited a small ZOI of 4.3 ± 0.30 mm, indicating a synergistic effect to the antifungal activity of the drug-loaded nanofiber. LCZ-loaded nanofibers can emerge as a novel approach for vaginal drug delivery in the treatment of candida infection. Thus, this pharmaceutical investigation can help in formulating preclinical and clinical models.
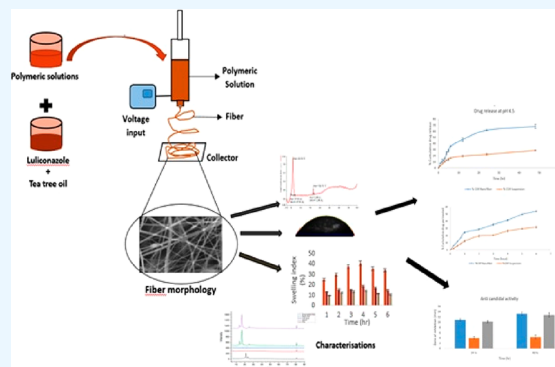
INTRODUCTION

Vaginal candida infection is a fungal disease caused by *Candida* yeast species that infects the lower genitalia of females in their reproductive age.[1,2] Vaginal candidiasis is predominantly caused by *Candida albicans,* which is responsible for 90−95% of the infections, and the rest are caused by nonalbicans species such as *C. glabrata, C. krusei, C. parapsilosis,* and *C. tropicalis.*[3,4] Worldwide, approximately three-fourths of females are affected at least once in their lifetime.[5] The maximum attack rate is found in young female adults (25−45 years old).[6] The vaginal candida infection can be identified by pruritis, erythema, burning sensation, painful coitus, white curd-like discharge, and hyperemia.[7] Triggering of the disease depends on the inconvenience in equilibrium between candida colonization in the vagina and the host condition.[8] Immunosuppression, overuse of antibiotics, diabetes, pregnancy, high estrogen

levels, change of vaginal pH, skin-fitting underwear, use of oral contraceptives, spermicides/condoms, and unhygienic habits are the major risk aspects for causing the disease.[9] Vaginal candidiasis causes financial and social burdens with a decline in QoL (quality of life) of the women instead of mortality. The available treatment is related to therapeutic constraints like low therapeutic efficacy that may lead to recurrence, poor bioavailability, flushing due to high content of vaginal
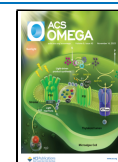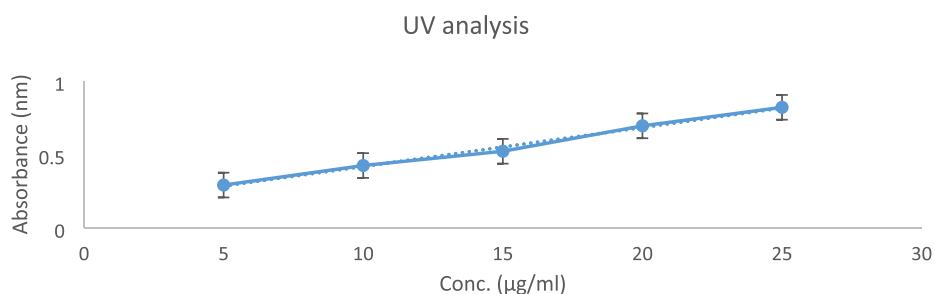
Figure 1. UV spectral analysis of luliconazole drug in SVF (pH 4.5).

Table 1. Binding Energies, RMSDs, Ligand Efficiencies, and Inhibition Coefficients of Luliconazole and Tea Tree Oil for Lanosterol 14-Alpha Demethylase

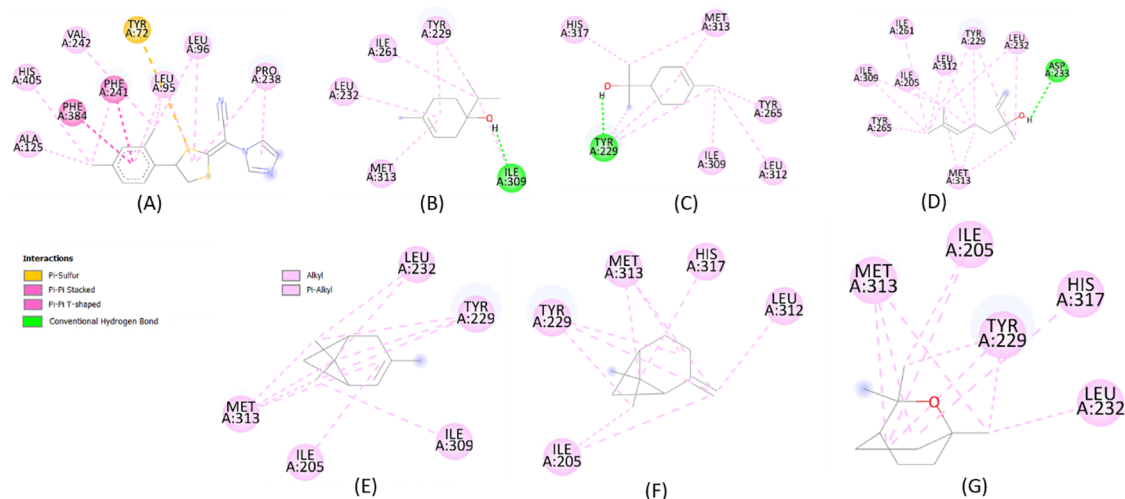| s. no.	protein	ligand	binding energy(kcal/mol)	cluster RMSD	ligand efficiency	inhibition coefficient
Antifungal activity						
1.	lanosterol 14-alpha demethylase (5HS1)	luliconazole	−8.70	0.00	−0.41	416.74 nM
Tea tree oil						
1.	lanosterol 14-alpha demethylase (5HS1)	terpinen-4-ol	−6.23	0.01	−0.57	27.21 μM
2.		α-terpineol	−6.31	0.01	−0.57	23.53 μM
3.		linalool	−5.10	0.00	−0.46	181.56 μM
4.		α-pinene	−6.02	0.00	−0.6	38.77 μM
5.		β-pinene	−6.10	0.00	−0.61	33.8 μM
6.		1,8-cineole	−5.85	0.00	−0.53	51.67 μM

Figure 2. 2D plot of ligand−protein interaction of (A) luliconazole, (B) terpine-4-ol, (C) alpha-terpineol, (D) linalool, (E) alpha-pinene, (F) beta-pinene, and (G) 1,8-cineole.

discharge, poor patient compliance, low adhesion to the vaginal mucosa, frequent dosing, and long duration of therapy.[10] To overcome the aforesaid challenges, a strategic formulation with improved therapeutic outcomes for eliminating and countering the recurrence of the disease is necessary.[11] Therefore, developing a novel system is required for localized drug delivery with a prolonged release in a single dose and enhanced fiber adhesion, retention, and drug penetration to the vaginal mucosa.[12] There is a dearth of evidence regarding luliconazole (LCZ) use in vaginal candidiasis treatment. Despite being a broad-spectrum antifungal drug, luliconazole has been especially used for the eradication of dermal, nail, and eye fungal infections.[13] Certain characteristics of LCZ mentioned in the published literature such as low inhibitory concentration (MIC range: 0.031−0.13 μg/mL), lipophilicity, powerful anticandidal activity, efficiency at very low concen-

tration, skin compatibility, and effective in silico study results made the drug a potential candidate to treat vaginal candidiasis.[14,15] Nanofibers are a newer polymeric nanosystem that delivers the drug by entrapping it into a web-like fibrous structure.[16] In addition, nanofibers exhibit a large surface area to volume ratio, enhanced drug loading capacity, capability to assimilate a wide variety of drugs, efficient drug release, and ease of fabrication, which are more convenient features over conventional formulations.[17,18] The accomplishment of any formulation depends on the approach, method, and components considered, such as the drug and excipients. PCL/gelatin fibers were prepared by the electrospinning method, and optimization was done using the Box−Behnken design (BBD). Tea tree oil, an essential oil of *Melaleuca alternifolia*, is considered as an active excipient for this current study. Additionally, it possesses an antifungal property that
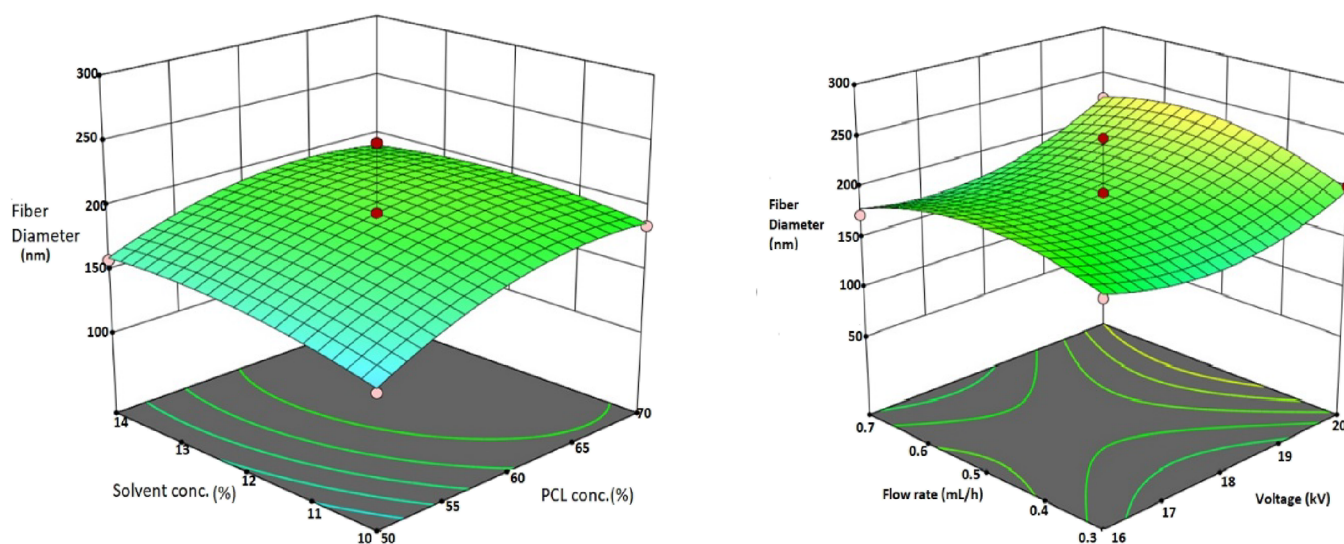
Figure 3. Contour plot showing influence of independent variables on dependent variables.

may give an enhanced effect to the anticandidal activity of luliconazole.[19] Fabricated nanofibers were analyzed during the characterization steps for investigating the suitability of LCZ in the treatment of vaginal candida infection. To the best of our knowledge, this is the first research that aims to design an LCZ-loaded nanofiber using the electrospinning technique to treat vaginal *C. albicans* infection.

RESULTS AND DISCUSSION

UV Analysis. The solubility of luliconazole drug in SVF pH 4.5 was estimated through UV analysis, and a satisfactory result was obtained[20] (Figure 1). An admissible solubility of the drug allowed its use for further formulation development.

In Silico Guided Selection of Excipients. We compared the binding energies of luliconazole with the six most important components of tee tree oil for the antifungal enzyme, i.e., lanosterol 14-alpha demethylase.[21] The binding energy values came out to be in the range of −5.10 to −8.70 kcal/mol. The docking data supported the fact that the components of tea tree oil also possess antifungal activity because of negative binding energies and one hydrogen bond found each in terpinene-4-ol, alpha terpineol, and linalool. All computed binding energies, RMSDs, ligand efficiencies, and inhibition coefficients are reported in Table 1.

Because the value of binding energy of tea tree oil was less negative than the standard luliconazole, the presence of hydrogen bonding in the tea tree component that was absent in luliconazole supports the fact that tea tree oil would show an enhanced effect with luliconazole for antifungal activity and be considered as an active excipient loaded in the formulation. Thus, tea tree oil would not only act as a bioavailability enhancer but also help in demonstrating pharmacological action. The 2D plots of ligand-protein interaction are shown in Figure 2.

Optimization of Nanofibers. To provide an efficient and cost-effective result, determining the process parameters is of the utmost importance. The traditional "one-factor-at-a-time strategy" is time-consuming and avoids interactions between independent variables, which opens the door for new optimization strategies. Response surface methodology (RSM) is a prospective optimization approach that enables

the determination of various parameters and their interactions with a minimum number of experimental runs.[22] This method attempts to anticipate the suitability of the model by analyzing the responses of interactions between statistically determined combinations and determining the coefficients of the best-fit model. The different samples were produced using the Design-Expert software, and results were obtained. PCL concentration, solvent concentration, flow rate, and voltage were chosen as the independent variables, and fiber diameter size (nm) was chosen as the dependent variable. On the basis of the interactions between the dependent and independent variables, polynomial quadratic equations and the corresponding correlations were developed. The analysis resulted in a contour plot that showed the qualitative effects of all the variables on response depicted in Figure 3.

The plots manifested that with an increase in PCL polymeric concentration, the viscosity of the solution increases, which leads to an increase in fiber diameter. In the case of solvent concentration, fiber diameter decreased with an increase in solvent concentration, showing the direct effect of the viscosity of the solution on the fiber diameter. The flow rate had a variable effect on the diameter of the fiber. The increase in voltage increased the fiber diameter, which may be due to the fact that a higher voltage leads to the ejection of more polymers from the needle, which causes a larger diameter. For the desired drug release profile, fiber diameter is one of the crucial parameters that are important to consider.[23] A smaller diameter shows a higher surface area with effective mass transfer.[24] By the influence of different variables, the mean diameter of prepared nanofibers obtained were in the range of 100 to 278 nm. The beadles and uniform fibers with a minimum diameter were taken into account for further studies. The second-order polynomial equation relating the response of fiber diameter (Y) is given below.

$$Y = 195 + 19.67A + 6.08B + 14.75C + 5.50D - 4.75AB$$
$$- 69.75AC + 16.00AD + 29.75BC - 11.75BD$$
$$+ 7.75CD - 17.54A^2 - 8.67B^2 + 25.08C^2$$
$$- 23.29D^2$$

Table 2. Analysis of Variance (ANOVA) for the Model

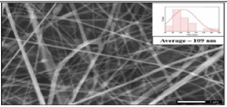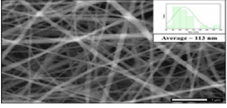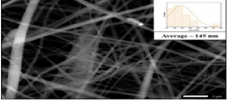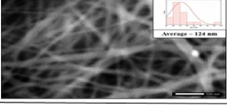| source	sum of squares	df	mean square	F value	P value probab > F	
model	44,826.77	14	3201.91	9.42	<0.0001	significant
A-PCL conc.	4641.33	1	4641.33	13.66	0.0024	
B- solvent conc.	444.08	1	444.08	1.31	0.2722	
C-voltage	2610.75	1	2610.75	7.68	0.0150	
D-flow rate	363.00	1	363.00	1.07	0.3189	
AB	90.25	1	90.25	0.27	0.6144	
AC	19,460.25	1	19,460.25	57.26	<0.0001	
AD	1024.00	1	1024.00	3.01	0.1045	
BC	3540.25	1	3540.25	10.42	0.0061	
BD	552.25	1	552.25	1.62	0.2232	
CD	240.25	1	240.25	0.71	0.4146	
A2	1995.96	1	1995.96	5.87	0.0295	
B2	487.21	1	487.21	1.43	0.2511	
C2	4081.13	1	4081.13	12.01	0.0038	
D2	3518.93	1	3518.93	10.35	0.0062	
residual	4757.92	14	339.85			
lack of fit	141.92	10	14.19	0.012	1.0000	not significant
pure error	4616.00	4	1154.00			
cor total	49584.69	28				
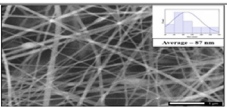
Positive coefficients show a direct relationship between variables and response, whereas negative coefficients show an inverse relationship between them. Analysis of variance (ANOVA) was used to know the statistical importance of the four factors and their interactions to get a mathematical model (Table 2).

The quadratic model with an F value of 9.42 implies significant model values, and "prob > F" less than 0.0500 indicates that model terms are significant. In this case A, C, AC, BC, A^2, C^2, and D^2 are significant model terms. The "lack of fit F value" of 0.01 implies that the lack of fit is not significant relative to the pure error. A nonsignificant lack of fit is good for the adequate fitting of data. The lack of fit test and model summary statistics suggested that the models are quadratic. The "pred R-squared" of 0.8381 is in acceptable agreement with the "adj R-squared" of 0.8081. In addition to this, the coefficient of variation with a value of 9.97 also indicated the reliability of the model with high precision. Therefore, the chosen quadratic model can be used to steer the design for nanofibers. The predicted diameter of fiber was 151.04 nm, and the actual experimental optimized fiber average diameter was found to be 153 nm. The lesser difference between the predicted and experimental values of fiber diameter exhibited the reliability of the BBD approach for the development of nanofibers.

Drug Loading and Morphology of Nanofibers Using Scanning Electron Microscopy (SEM). The optimum PCL/gelatin blank nanofibers were prepared, and then the tea tree oil loaded at different concentrations (2.5, 5, 7.5, and 10%) led to the production of nanofibers of different diameters. The morphological structure of these nanofibers loaded with tea tree oil was observed under SEM, which revealed that with an increase in concentrations of TT oil, the diameter of nanofibers increases. The average diameters of 2.5, 5, 7.5, and 10% TT oil-loaded fibers were 87 ± 34, 109 ± 41, 113 ± 48, and 145 ± 47 nm, respectively, as shown in Table 3.

Among all, the fiber with oil in 7.5% concentration was found to be bead-free and more uniform with an average diameter of 113 ± 48 nm and was considered the best one, so it can be an optimal choice for drug loading. Then the loading

Table 3. Analysis of SEM Images of PCL-Gelatin/Tea Tree Oil Nanofiber Mats[a]

Samples	SEM images	Average diameter
PCL/gelatin nanofiber with 2.5% tea tree oil		87nm ± 34
PCL/gelatin nanofiber with 5% tea tree oil		109 nm ± 41
PCL/gelatin nanofiber with 7.5% tea tree oil		113 nm ± 48
PCL/gelatin nanofiber with 10% tea tree oil		145 nm ± 37
PCL/gelatin- oil nanofiber with luliconazole drug		124 nm ± 37

[a]Table 3 is entirely original.

of luliconazole drug (5% with respect to the polymeric solution) was carried out, and a drug-loaded nanofiber was produced that exhibited an average diameter of 124 ± 37 nm. The packing of luliconazole drug in the fiber increased the fiber strength, and the morphology of drug-loaded fiber revealed its rough surface, which indicates the presence of some amount of drug on the fiber surface. The morphology of optimized blank, TT oil-loaded, and LCZ-loaded nanofibers is shown in Figure 4a−c, respectively.

FTIR Analysis. FTIR analysis was performed to determine the existence of any interaction between excipients and drug and also to know the influence of the electrospinning technique over the functional groups in the nanofibers.[25] The different FTIR spectrum overlays are presented in Figure 5. Luliconazole showed characteristic peaks at 3039 cm^{-1}
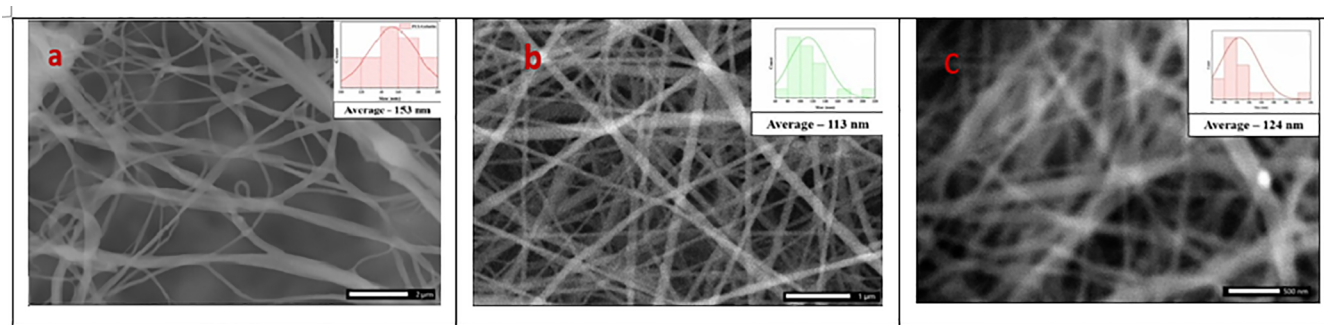
Figure 4. SEM images of (a) PCL/gelatin nanofiber, (b) 7.5% TT oil-loaded fiber, and (c) LCZ-loaded nanofiber.
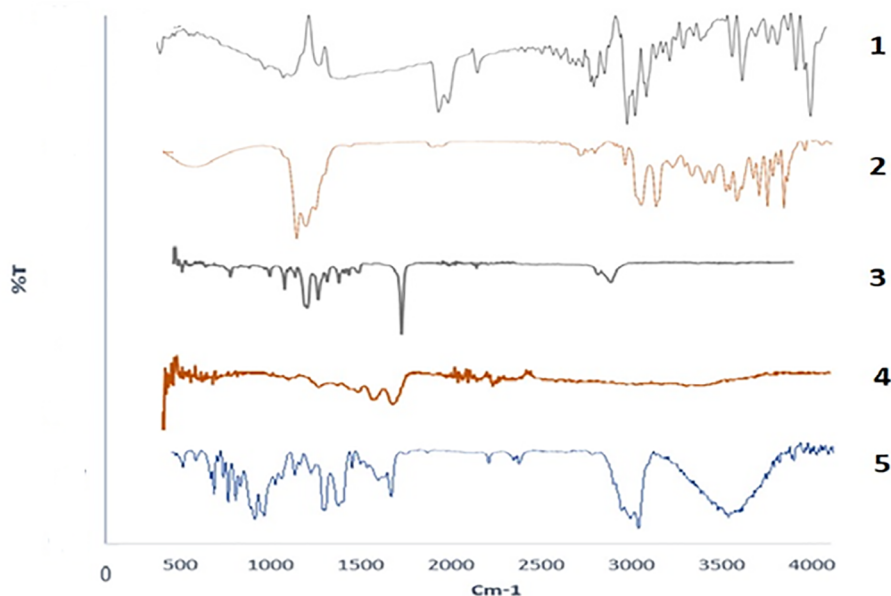

Figure 5. FTIR spectra of (1) luliconazole drug, (2) tea tree oil, (3) polycaprolactone, (4) gelatin, and (5) LCZ-loaded nanofiber.

(aromatic C−H stretching), 2941 cm^{-1} (C−H aliphatic stretching), 2527 cm^{-1} (S−H stretching), 2199 cm^{-1} (CΞN stretching), 1698 cm^{-1} (C=C alkene stretching), and 1634 cm^{-1} (C=N stretching). Tea tree oil had distinctive peaks at 3362 cm^{-1} (O−H bonding), 2855 cm^{-1} (−CH3 group), and 1025 cm^{-1} (C−O bond). PCL showed its characteristic peaks at 1727 cm^{-1} (C=O stretching), 2865 cm^{-1} (symmetric CH2 stretching), and 2948 cm^{-1} (asymmetric CH2 stretching). Gelatin exhibited peaks at 1640 cm^{-1} (C=O stretching) and 1543 cm^{-1} (N−H bending). FTIR spectra of drug-loaded nanofiber appeared with all the characteristic peaks of PCL, gelatin, tea tree oil, and luliconazole with negligible changes in frequencies, which proved that there is no interaction between the drug and excipients in the formulation and also proved that the electrospinning process had no effect on the excipients as well as on the drug present within the nanofiber.

Differential Scanning Calorimetry Analysis. DSC studies were performed to check the compatibility and the thermal behavior of excipients and drug, which were assessed through thermograms.[26] Compatibility is expected if different peaks of excipients and the drug remain the same in the thermogram, or if the peak disappears, the substance may be thought to be amorphous. In Figure 6a, PCL shows its characteristic peak at 64.1 °C, and gelatin shows its degradation peak at 300.8 °C in Figure 6b. In Figure 6c, a sharp endothermic peak at 152 °C was observed in the

thermogram, which indicates the melting point of LCZ. In the drug-loaded nanofiber formulation (Figure 6d), the presence of a PCL peak with a slight change is seen, which shows the stability of the polymer in the formulation, whereas the absence of a degradation peak of gelatin in the nanofiber also represents the stability of gelatin. The absence of the characteristic peak of the luliconazole drug in the nanofiber shows that the LCZ was amorphous by the loading of LCZ in the nanofiber.

XRD Analysis. X-ray diffraction reveals the crystallinity and amorphous form of the drug and polymers. XRD of PCL, gelatin, luliconazole, blank nanofiber, and LCZ-loaded nanofiber is displayed in Figure 7. PCL exhibited its two characteristic peaks at 21.2 and 23.6° that specify the crystalline nature of PCL. Gelatin with no specific peak reveals its amorphous nature. Pure LCZ showed very low-intensity peaks at 15.6, 17.5, 20.6, 21.1, 22.6, 23.8, and 25.0°, which specify the crystallinity of the drug. The blank nanofiber showed the specific peaks of the excipients, which signalizes the preserved characteristic nature of excipients in the fiber. In drug-loaded nanofibers, specific peaks of the drug disappeared, indicating that the distribution of the amorphous phase of the drug in the fiber leads to higher solubility of the drug in the vaginal fluid and would be beneficial for drug delivery.

Degree of Swelling. The swelling of nanofibers has its significance in the drug release through the process of diffusion
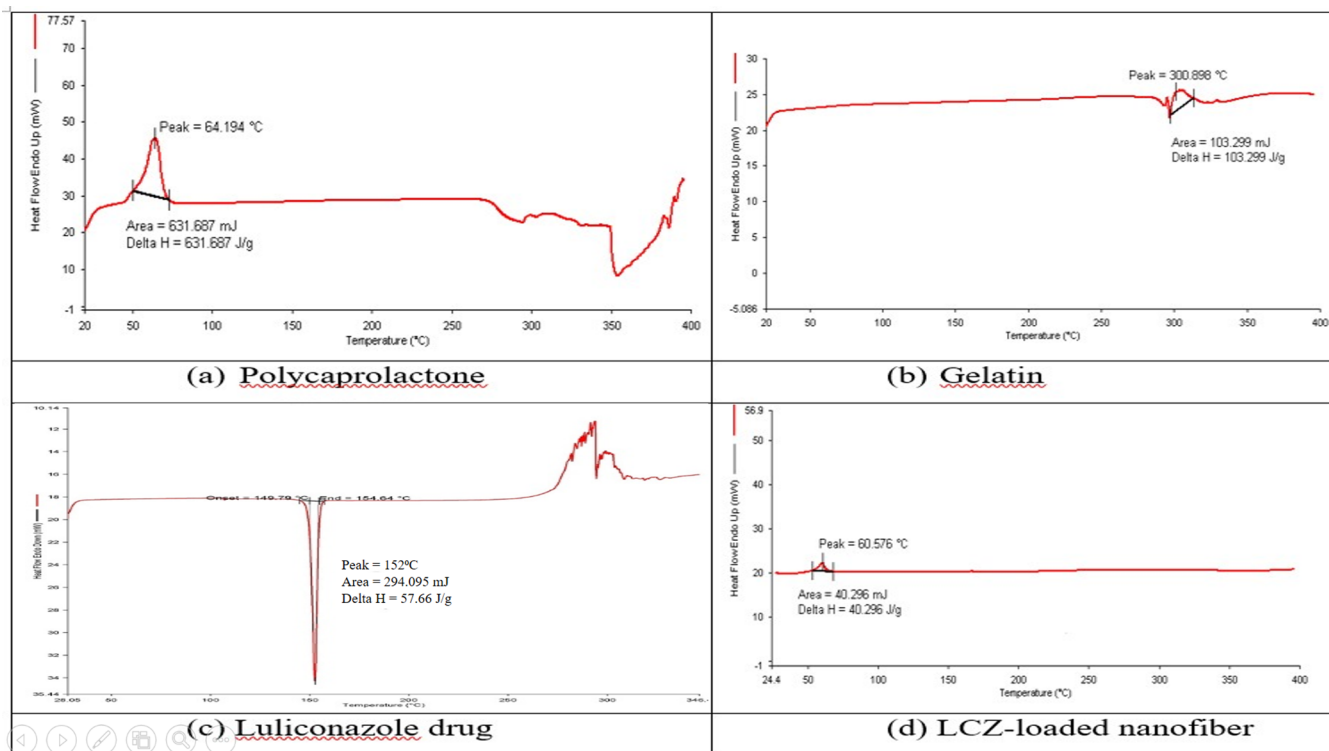
Figure 6. DSC curves of (a) polycaprolactone, (b) gelatin, (c) luliconazole drug, and (d) LCZ-loaded nanofiber.
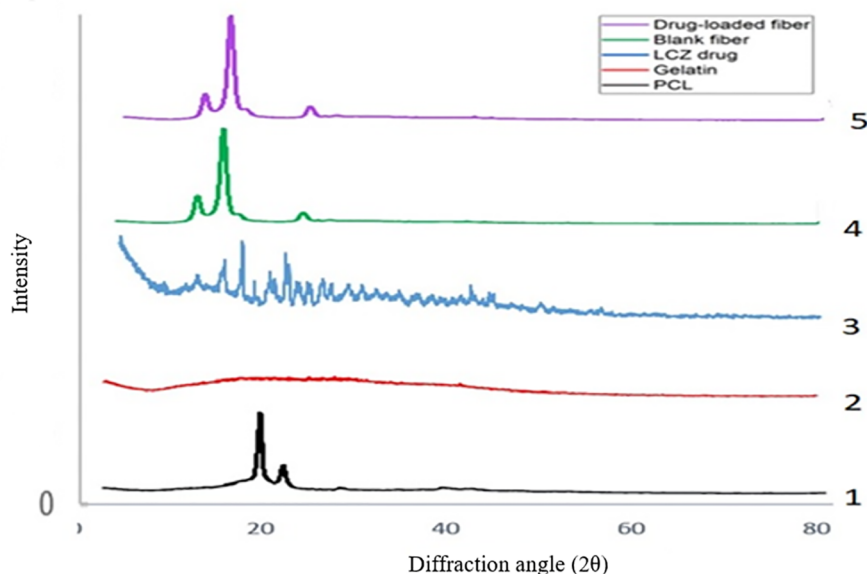

Figure 7. XRD pattern of (1) PCL, (2) gelatin, (3) LCZ drug, (4) blank nanofiber, and (5) LCZ-loaded nanofiber.

of the drug particles and also facilitates the release pattern of the drug.[27] The swelling degree of nanofibers was examined for 6 h at room temperature in SVF pH 4.5, and results are shown in Figure 8. After 1 h, the swelling degree was found to be 25, 13.1, and 9.5% for blank, fiber with tea tree oil, and drug-loaded nanofiber, respectively. A maximum increment in the swelling was obtained at 4 h, i.e., 40.8, 18.9, and 14.0% for blank, fiber with TT oil, and drug-loaded nanofiber, respectively. A decrease in swelling degree was noticed after 4 h which may be due to the initiation of polymer erosion or degradation from the fiber. From the results, it is decoded that the blank nanofiber swelled more in comparison to the fiber

with TT oil and LCZ-loaded nanofiber. This reveals the hydrophobicity of TT oil and luliconazole drug that decreased the swelling property of the fiber. PCL is a hydrophobic polymer but when blended with a highly hydrophilic polymer gelatin forms a hydrophilic composite. Gelatin swells and decreases the porosity of the fiber which results in a slower release or diffusion of the drug from the fiber. When the nanofiber is applied at the vaginal site, the fiber swells because of the release of vaginal fluid and facilitates the release of the drug in the vagina.

Entrapment Efficiency. Entrapment efficiency indicates the amount of drug that gets entrapped into the fibers. It can
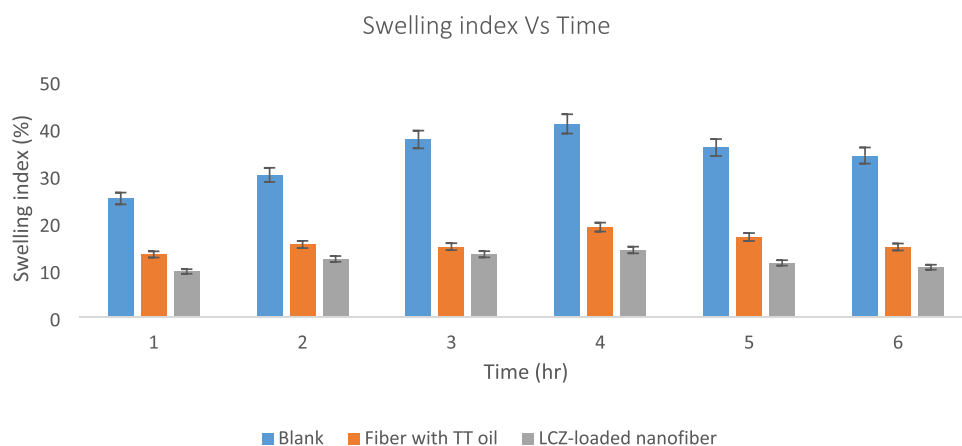
Swelling index Vs Time

Figure 8. Swelling index of the blank nanofiber, nanofiber with TT oil, and LCZ-loaded nanofiber at different time intervals.
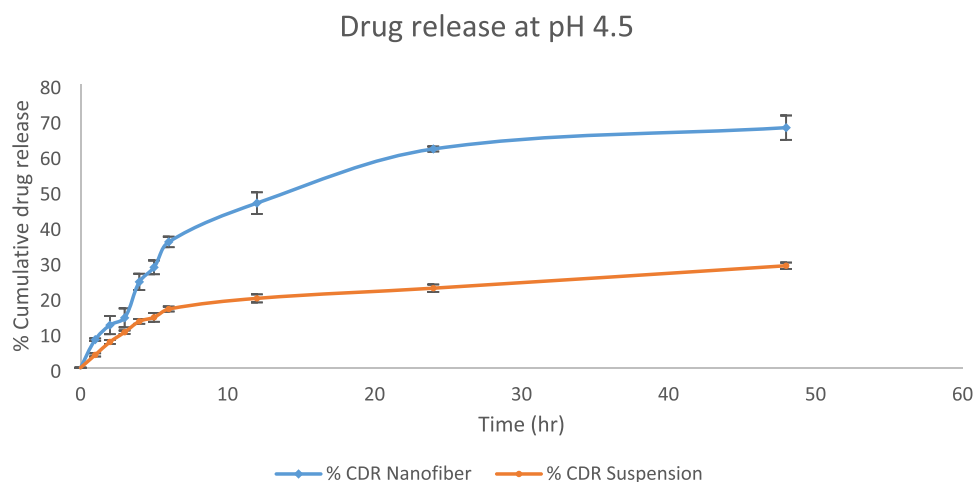
Drug release at pH 4.5

Figure 9. In vitro drug release profile of the drug-loaded nanofiber and drug suspension.

affect the dose of the drug that is to be delivered at the targeted site to treat the disease and to ensure the effectiveness of the drug-loaded fibers.[28] The entrapment efficiency of the drug-loaded nanofiber was found to be $89.2 \pm 0.8\%$. The small decrease in the amount of drug entrapped may be due to the improper collection of fibers on the collector. A part of the nanofibers may be collected on the other part of the collecting device during the electrospinning process. The resultant EE (%) of the nanofiber was found to be satisfactory because the amount of drug entrapped is more than the minimum inhibitory concentration against *C. albicans* (MIC of LCZ against *C. albicans*: $0.031-0.13 \mu g/mL$), so it can be used for optimum antifungal activity at the vaginal site.

Contact Angle. The contact angle measurement is significant to know the extent of wettability of the nanofibers.[29] The contact angle of the PCL/gelatin nanofiber was found to be $46.5°$, which implies the hydrophilic nature of the fiber. The addition of gelatin to the PCL increases the hydrophilicity of the fiber as a result of the presence of a large number of hydrophilic amino acids in the gelatin. The contact angles of nanofiber with tea tree oil and LCZ-loaded nanofiber were found to be $62.95°$ and $65.78°$, respectively. This hike in contact angle of the drug-loaded nanofiber in comparison to that of the blank nanofiber is attributed to the hydrophobic nature of TT oil and LCZ drug. The contact angles of the formulated nanofibers depicted their hydrophilic nature. The measured contact angle of $65.78°$ of the drug-loaded nanofiber

showed hydrophilicity. Therefore, it facilitates the wettability of nanofibers with vaginal fluid and increases the contact surface of fiber to the vaginal mucosa, which will help in the delivery of drug at the site.

Mucoadhesive Test. Mucoadhesive force facilitates the contact between the formulation and the vaginal mucosal site for a better residence time. The mucoadhesive force of the blank nanofiber, TT oil-loaded nanofiber, and LCZ-loaded nanofiber was obtained as 0.10, 0.04, and 0.03 N, respectively. The lower mucoadhesive force of the TT oil-loaded fiber and LCZ-loaded fiber than that of the blank fiber was attributed to the hydrophobic nature of TT oil and luliconazole that lowered the hydrophilicity of the fibers in comparison to the blank fiber. We found a decrease in the wettability in the drug-loaded nanofiber, but it is only up to a certain extent because it shows a satisfactory mucoadhesive force value that will facilitate the adhesion and residence time of the LCZ-loaded nanofiber to the vaginal surface that help in drug release for a prolonged time.

Tensile Strength. The mechanical strength of the blank nanofiber, TT oil-loaded fiber, and drug-loaded nanofiber was 0.187, 0.148, and 0.445 N/m. The lowest tensile strength was found in the case of the TT oil-loaded fiber, which was attributed to the fluid property of TT oil that reduces the strength of the fiber. The drug-loaded nanofiber had a higher tensile strength than the blank and TT oil-loaded fiber which indicates the packing of the drug inside the meshes of drug-
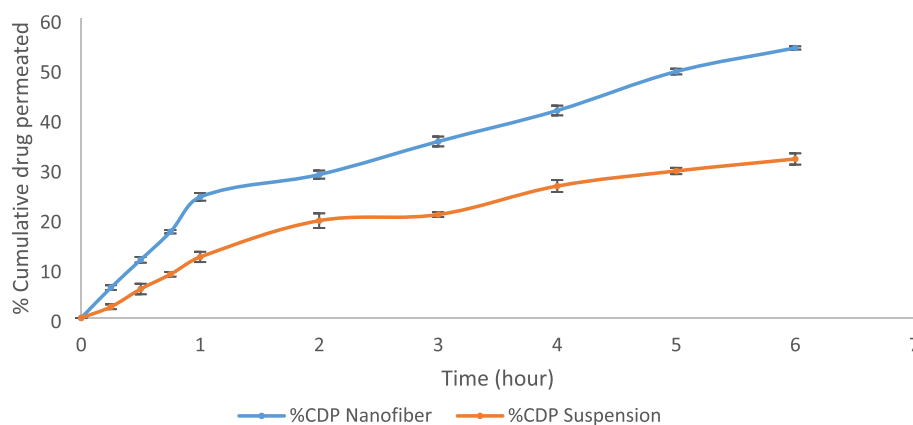
Figure 10. Permeation profiles of the nanofiber and suspension through goat vaginal mucosa.
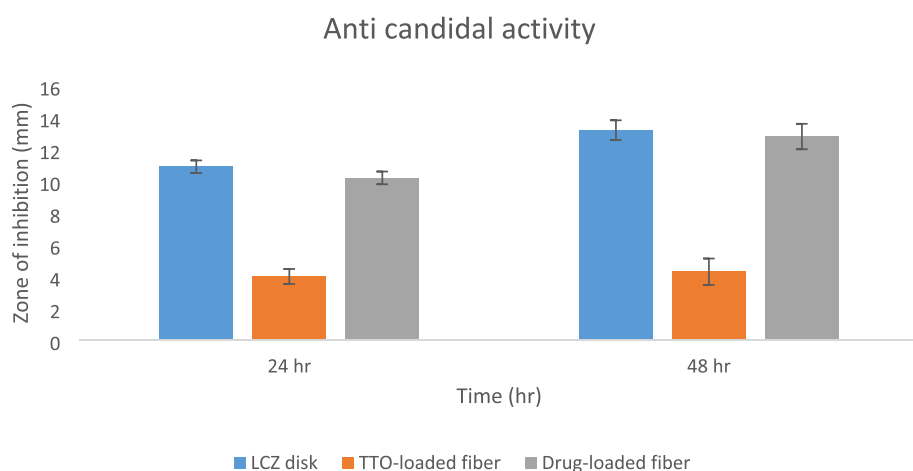

Figure 11. Anticandidal activity possessed by different nanofiber mats and the LCZ disk.

loaded fiber, increase fiber density and hence increases the tensile strength of the fiber, which minimizes the tear of fiber at the site of application.

In Vitro Drug Release Study. The in vitro drug release profile of the LCZ-loaded nanofiber and LCZ suspension was analyzed and is illustrated in Figure 9. A release of $7.9 \pm 0.33\%$ of the drug from the nanofiber was observed within the 1 h of the study that reached $67.7 \pm 3.4\%$ after 48 h of study, which was found to be more than the release of drug from the suspension. The increment of drug release in case of nanofibers occurred because of the formation of nano range of fibers. The enhanced availability of drugs in the dissolved state could lead to better absorption and hence bioavailability. The results obtained through in vitro release data showed the enhanced solubility of the luliconazole drug in the developed nanofiber. In addition, kinetics and the mechanism of drug release were derived by fitting the release data in different kinetic models. After kinetic modeling, data of drug release were best addressed by the Korsmeyer–Peppas model, which expressed the highest R-square value ($R^2 = 0.921$) compared to other models. The diffusion coefficient (n) value for the Korsmeyer–Peppas model was less than 0.5, which revealed the diffusion mechanism of drug release.

Ex Vivo Permeation Study. The ex vivo permeation study showed that the permeation of the luliconazole drug was augmented with PCL/gelatin nanofibers from vaginal mucosa as compared to a suspension (Figure 10). The percentage cumulative drug permeation was found as $54.13 \pm 0.32\%$

within 6 h and $31.87 \pm 1.13\%$ for the suspension. As the PCL/gelatin nanofiber is a hydrophilic composite, it will improve the wettability of LCZ in the vagina. The adequate penetration may be due to the diameter of fiber in the nano range and also the use of tea tree oil that helped as a penetration enhancer. Therefore, the study proved that the drug-loaded nanofiber was suitable for application in the vagina.

Anticandidal Activity. The anticandidal activity exhibited by the nanofiber and LCZ disk is shown in Figure 11. The zone of inhibition (ZOI) of the luliconazole-loaded nanofiber was 12.8 ± 0.53 mm after 48 h, which revealed the potential to inhibit *C. albicans*. The TTO-loaded nanofiber possessed a small ZOI of 4.3 ± 0.30 mm, indicating its anticandidal activity. The LCZ disk showed a ZOI of 13.2 ± 0.62. The ZOI of the nanofiber was found to be closer to the ZOI of the LCZ disk, which means that drug-loaded nanofiber also possesses anticandidal activity that could help in the eradication of *C. albicans* at the vagina. This demonstrates that TT oil added with LCZ in the nanofiber as an excipient may also provide an enhanced effect on its anticandidal capability. The blank fiber showed no ZOI against *C. albicans*. From the results, it can be explained that electrospinning does not affect the anticandidal activity of luliconazole and LCZ-loaded nanofiber can be used as a better tool for the eradication of *C. albicans* infection.

CONCLUSIONS

In this study, luliconazole-loaded PCL/gelatin nanofibers were fabricated through an electrospinning technique for the treatment of vaginal candida infection. The morphology of the nanofibers and their diameter were determined. The optimization of fibers derived the nanofiber with a minimum diameter and beadless morphology. FTIR spectroscopy and DSC analysis of nanofibers showed that no interaction exists between the drug and excipients and LCZ was successfully loaded into the nanofibers. The XRD analysis showed the distribution of the amorphous phase of the luliconazole in the nanofibers that eased the delivery of LCZ. The swelling degree revealed that with an increase in the hydrophobicity, the swelling of nanofibers decreases. The swelling of nanofibers also facilitates the release of drug by diffusion of drug particles from the fiber mesh. The contact angle test depicted the wettability and hydrophilicity of the LCZ-loaded nanofiber that increased the contact surface of the fiber to the vaginal mucosa. Mucoadhesion was found to be satisfactory, which enhanced the residence time of nanofibers, and the better tensile strength prevented its tear at the application site. The release of the drug from the formulation showed sustained action, and release kinetics followed the Korsmeyer–Peppas model. The release of luliconazole from the LCZ-loaded nanofiber happened through the Fickian release. Entrapment of luliconazole in nanofibers enhanced the permeation in the vaginal mucosa in comparison to the drug suspension. The microbiological assay and in silico activity proved the anticandidal activity. Therefore, this research detailed a luliconazole nanofiber fabricated for the first time that could successfully work in the anticandidal action for the management of vaginal candidiasis.

MATERIALS AND METHODS

Materials. PCL (average molecular weight 80,000) and gelatin (Type A porcine skin, 75–100 bloom) were procured from Sigma-Aldrich, USA. The luliconazole drug and tea tree oil were purchased from Eyaan Pharmaceuticals, New Delhi, India. The solvents used were analytical grade. *Candida albicans* were obtained from the Department of Microbiology, Ram Manohar Lohia Hospital, New Delhi.

Estimation of the Drug by UV Analysis in SVF. Drug solubility and stability were checked by preparing fresh simulated vaginal fluid (SVF) at pH 4.5. The stock solution of the drug in SVF was prepared by the addition of 10 mg of the drug in the mixture of 5 mL of methanol and 5 mL of SVF. Then sequential dilutions of 5, 10, 15, 20, and 25 μg/mL were prepared using SVF and were analyzed using a UV spectrometer at λ_{max} 299 nm.[20]

In Silico study. *Ligand Preparation.* Luliconazole and tee tree oil were used as the ligand molecules in this study. Their 3D structures were downloaded from the PubChem database (http://pubchem.ncbi.nlm.nih.gov) in .sdf format. This was further converted into .pdb format by using the OpenBabel software. The .pdb file of the ligand was converted into .pdbqt format by Autodock Tools 1.5.6.

Protein Preparation. The RCSB (Research Collaboratory for Structural Bioinformatics) protein databank is a digital depository for the 3D structures of different protein molecules (http://www.rcsb.org). Structures of lanosterol 14-alpha demethylase (PDB ID: 5HS1) enzyme has been downloaded from the RCSB site for investigating the antifungal activity.[29]

The enzyme structures were retrieved from RCSB in .pdb format. Further processing of the structures was done by deleting the water molecules, adding polar hydrogen molecules, and adding Kollman charges in Autodock Tools 1.5.6. The processed structures were saved in .pdbqt format.

Docking Study Using AutoDock 1.5.6. The energy-minimized structures of both the ligand and protein in .pdbqt format were docked by inserting them into Autodock Tools 1.5.6. For docking, the entire structure of the protein was enclosed inside a grid box with a grid spacing of 1 Å. The protein structure was kept rigid, whereas the ligand molecule was kept flexible to find the pose with minimum binding energy. Flexible anchoring to the active site receptor was determined by using the Lamarckian genetic algorithm. The binding site was added, and the interaction energy between the ligand and receptor was calculated for the entire binding site and expressed as affinity (kcal/mol). The results of the docking were regrouped at a tolerance of 4.0 Å root-mean-square deviation (RMSD)

Protein–Ligand Interactions. Discovery Studio 2021 client was used for studying the interactions between the ligand and the protein molecule. The 2D structures of the interactions are shown in Figure 2. The hydrogen bonds were shown by green dotted lines, whereas other bonds were also represented by different colors.

Fabrication and Optimization of the Nanofiber. *a) Method of Fabrication of the Nanofiber by Electrospinning.* Polymeric solutions of PCL/gelatin were produced in three different ratios, i.e., 50:50, 60:40, and 70:30, in 2% acetic acid solvent and formic acid (3:1) in ratios of 8, 10, and 12%. Fibers of PCL/gelatin were fabricated with an electrospinning technique that involved the insertion of polymeric solution in the syringe needle attached to the pump and voltage generator. The flow rates were 0.3, 0.5, and 0.7 mL/h, and voltages of 16, 18, and 20 kV were considered. The polymeric solution formed a jet when ejected from the needle and then collected on the aluminum foil.

b) Optimization of Nanofibers through the BBD Approach. The Box–Behnken design (BBD) was utilized in this research work to get the minimum mean fiber diameter by changing the values of different independent variables. For optimization purposes, four variables were selected such as PCL concentration, solvent concentration, voltage applied, and flow rate in a range of three levels (−1, 0, and 1). The independent as well as dependent variables that were considered for optimization with their expected goals are depicted in Table 4.

Table 4. Experimental Factors with Their Range and Levels for Optimization of PCL/Gelatin Nanofibers

variables	factors	unit	level of variables		
			−1	0	1
Independent variables					
PCL concentration	A	% wt	50	60	70
solvent concentration	B	%	10	12	14
voltage	C	kV	16	18	20
flow rate	D	mL/h	0.3	0.5	0.7
Dependent variable					
average fiber diameter	Y	nm	**goal:** minimize		

A total of 29 samples were generated through the BBD using the Design-Expert software (13.0.14.0 Design-Expert 13) for further analysis (Table 5).

Table 5. Responses of Different Input Factors for the Average Diameter of PCL/Gelatin Nanofibers

formulation code	A PCL conc. (%)	B solvent conc. (%)	C voltage (kV)	D flow rate (mL/h)	Y average fiber diameter (nm)
F1	50	12	20	0.50	268
F2	60	12	20	0.30	201
F3	60	14	20	0.50	260
F4	60	12	20	0.70	224
F5	70	12	16	0.50	278
F6	60	14	18	0.30	176
F7	50	12	18	0.70	127
F8	60	12	18	0.50	195
F9	60	10	18	0.30	140
F10	50	10	18	0.50	135
F11	60	12	18	0.50	157
F12	**70**	**12**	**18**	**0.30**	**153**
F13	70	14	18	0.50	189
F14	70	12	20	0.50	167
F15	50	12	18	0.30	145
F16	60	14	18	0.70	164
F17	60	12	18	0.50	179
F18	70	10	18	0.50	185
F19	60	10	18	0.70	175
F20	60	12	18	0.50	249
F21	60	10	20	0.50	190
F22	50	14	18	0.50	158
F23	60	12	16	0.70	173
F24	60	12	18	0.50	195
F25	60	14	16	0.50	176
F26	60	12	16	0.30	181
F27	60	10	16	0.50	225
F28	70	12	18	0.70	198
F29	50	12	16	0.50	100

Drug Loading in the Optimized Nanofiber. Tea tree oil was taken in different concentrations, i.e., 2.5, 5, 7.5, and 10%, which were added to the optimum polymer blend for further nanofiber preparation. The concentration at which a uniform fiber with minimum diameter formed was selected for further drug loading. The luliconazole drug (5% with respect to the polymeric solution) was mixed in tea tree oil and then added to the polymeric solution. The mixture was stirred for 12 hours at room temperature. The prepared solution was electrospun at different variables considered. Electrospun nanofibers were obtained on an aluminum foil and dried at room temperature.

Characterization of Electrospun Nanofibers. *SEM Analysis.* The morphology and diameter of electrospun nanofibers were examined through SEM (Jeol, Japan). A small part of the fiber was cut and coated with a thin layer of gold and then placed over the sample holder of SEM. Magnified images from different positions were taken, and the average diameter was calculated.[30]

FTIR Analysis. The small pieces of electrospun nanofibers were cut and mixed with KBr to make small pellets. The spectrum was recorded between 400 and 4000 cm^{-1} wavelength range and at a resolution of 2 cm^{-1}. The interaction between the drug and excipients were determined.[31]

Differential Scanning Calorimetry Analysis. Drug-loaded nanofibers were analyzed for the thermal stability of the drug and excipients used. This study was carried out by weighing 2 mg of the sample placing it in a crucible and pressed it with a pressing machine. The crucible containing the sample was placed in the DSC instrument, and then sample was heated over a temperature range of 30 to 400 °C with a 10 °C/min heating rate under a nitrogen atmosphere.[31]

XRD Analysis. Samples were scanned with a speed of 2 °C/min at 37 °C using an X-ray diffractometer. The data were collected from $2\theta° = 0$ to $2\theta° = 80°$ intervals using a Rigaku, Japan, SmartLab 9 kW instrument.[32]

Degree of Swelling. The three dried nanofiber samples, i.e., blank, TT oil-loaded, and LCZ-loaded, were cut and weighed. Then these samples were immersed in SVF at pH 4.5 at room temperature. Samples were weighed at different time intervals for 6 h, and readings were noted. The degree of swelling was determined by using the following formula:

$$\text{Degree of swelling}(\%) = (W - W_\text{d})/W_\text{d} \times 100$$

where W is the weight of swollen nanofiber sample and W_d is the weight of the dried nanofiber sample.[33]

Entrapment Efficiency. The drug-loaded nanofiber of a known area (1×1 cm) was cut and dissolved in SVF pH 4.5. The solution formed was centrifuged, and the drug amount in the solution was determined by using a UV spectrophotometer instrument.[34] The estimation of the drug entrapment efficiency of the nanofiber was carried out by using the formula:

$$\text{Entrapment efficiency}(\%)$$
$$= \text{actual amount of drug/therapeutic amount of drug}$$
$$\times 100$$

Contact Angle. To monitor the wettability of the fiber, contact angles were measured by a Dataphysics, Germany, OCAH 230 instrument using an SVF pH 4.5 on nanofiber samples at room temperature. The static drop volume of 5 μL was kept the same in all samples using a microsyringe. Contact angles were measured for each single drop at specific time intervals, and the measurements were taken as snapshots.[35]

Mucoadhesive Test. The mucoadhesive strength of nanofibers was measured by using a texture analyzer (5 kg loaded cells, TA.XT plus, Stable Micro Systems, UK). A piece of 1.5 cm of the nanofiber sample was attached to the attachment of instrument with a double-sided tape, and a piece of vaginal mucosa of the goat was fixed to the other side. Both of these attachments were kept in contact for 15 seconds by applying a triggering force of 5 g. Then the adhesive force between the fiber and vaginal mucosa was calculated.[36]

Tensile Strength. The tensile strength of the nanofiber was calculated using a texture analyzer (TA.XT plus, Stable Micro Systems, UK). The nanofiber with a length of 5 cm and a width of 2 cm was set in the tensile grip of the instrument. The nanofiber sample was stretched with an upper movable button by applying a triggering force of 5 g, and the force required to tear the fiber into two parts was calculated.[37]

In Vitro Drug Release Study. For the determination of drug release of the nanofiber, a piece of nanofiber mat (1×1 cm^2) was weighed and dipped in 100 mL of SVF (pH 4.5) media in a shaker incubator. A temperature of 37 ± 0.5 °C with 75 rpm was maintained for the study. Five milliliter aliquots were withdrawn at different time intervals, and 5 mL of fresh media

was added after every withdrawal to maintain the sink condition. The concentration of the drug present in the aliquots was determined by using a UV-spectrophotometer at λ_{max} of 299 nm. The percentage cumulative drug release of the optimized drug-loaded nanofiber sample was calculated.[38,39]

To illustrate the drug release kinetics, the data of drug release were arranged and fitted into different mathematical models such as first order, zero order, Higuchi, Hixon–Crowell, and Korsmeyer–Peppas.[40]

Ex Vivo Permeation Study. The ex vivo permeation study was carried out using Franz diffusion cells. The vaginal mucosa of the goat was used for the study. The SVF pH 4.5 buffer was kept in the receptor compartment of Franz cells. The vaginal tissue was pressed in between the donor and receptor compartment, and the drug-loaded nanofiber was kept in the donor compartment of the Franz diffusion cell. At different time intervals, 2.5 mL of the sample from the receptor compartment was withdrawn, and the same volume of fresh SVF was poured into the receptor compartment. The concentration of drug obtained after permeation through the vaginal mucosa was measured spectrophotometrically at 299 nm. Graphs were plotted for the cumulative amount of drug permeated vs time.[31]

Anticandidal Activity. The disk-diffusion method was chosen for the microbiological study. Sabouraud dextrose agar (SDA) media were prepared, sterilized (autoclaving), and placed in Petri plates for inoculation. The *C. albicans* strain (obtained from the Department of Microbiology, Ram Manohar Lohia Hospital, New Delhi) was streaked over the SDA plates and left for overnight growth. LCZ-impregnated disk and nanofiber samples were cut of the same weight/shape and placed over the SDA plate. These plates were kept for incubation at 37 ± 0.5 °C for 2 days. Fungal growth was observed in the plates, and the zone of inhibition was measured using a Vernier caliper.[41]

■ AUTHOR INFORMATION

Corresponding Authors

Suhel Parvez — *Department of Toxicology, School of Chemical and Life Sciences, Jamia Hamdard, New Delhi 110062, India;* ● orcid.org/0000-0002-6318-6506; Email: sparvez@jamiahamdard.ac.in

Kanchan Kohli — *Department of Pharmaceutics, School of Pharmaceutical Education and Research, Jamia Hamdard, New Delhi 110062, India; Director, Research & Publication, Lloyd Institute of Management and Technology (Pharm.), Greater Noida, Uttar Pradesh 201306, India;* ● orcid.org/0009-0007-0201-0383; Email: kanchankohli50@gmail.com

Authors

Arya Vidyadhari — *Department of Pharmaceutics, School of Pharmaceutical Education and Research, Jamia Hamdard, New Delhi 110062, India*

Nidhi Singh — *Department of Pharmaceutics, National Institute of Pharmaceutical Education and Research (NIPER), Kolkata, Jadavpur 700032, India*

Avinash Kumar Singh — *Department of Pharmaceutical Medicine (Division of Pharmacology), School of Pharmaceutical Education & Research, Jamia Hamdard, New Delhi 110062, India*

Tanya Ralli — *Department of Pharmaceutics, School of Pharmaceutical Education and Research, Jamia Hamdard, New Delhi 110062, India*

Pratima Solanki — *Special Centre for Nanoscience, Jawaharlal Nehru University, New Delhi 110067, India*

M Aamir Mirza — *Department of Pharmaceutics, School of Pharmaceutical Education and Research, Jamia Hamdard, New Delhi 110062, India*

Complete contact information is available at:
https://pubs.acs.org/10.1021/acsomega.3c02141

Author Contributions

Arya Vidyadhari: draft of the work, analysis and interpretation of data; Nidhi Singh: analysis of data; Avinash Kumar Singh: analysis of data; Tanya Ralli: interpretation of data; Pratima Solanki: design and optimization of fiber; M Aamir Mirza: revised the work, final approval; Suhel Parvez: revised all aspects of the work, final approval; Kanchan Kohli: design the work, final approval.

Notes

The authors declare no competing financial interest.

This study did not require any ethical approval or informed consent for studies with human or animal subjects because this study included only the use of instruments.

The data for publication will be available after request.

■ REFERENCES

(1) Zeng, X.; Zhang, Y.; Zhang, T.; Xue, Y.; Xu, H.; An, R. Risk factors of vulvovaginal candidiasis among women of reproductive age in Xi'an: a cross-sectional study. *BioMed Res. Int.* **2018**, *2018*, 9703754.

(2) Sobel, J. D. Pathogenesis of recurrent vulvovaginal candidiasis. *Curr. Infect. Dis. Rep.* **2002**, *4* (6), 514–519.

(3) Bradford, L. L.; Ravel, J.; Bruno, V. Understanding vulvovaginal candidiasis through a community genomics approach. *Curr. Fungal Infect. Rep.* **2013**, 7, 126–131.

(4) Krcmery, V.; Barnes, A. J. Non-albicans Candida spp. causing fungaemia: pathogenicity and antifungal resistance. *J. Hosp. Infect.* **2002**, *50* (4), 243–260.

(5) Gupta, S.; Kakkar, V.; Bhushan, I. Crosstalk between vaginal microbiome and female health: a review. *Microb. Pathog.* **2019**, *136*, No. 103696.

(6) Oparaugo, C. T.; Iwalokun, B. A.; Nwaokorie, F. O.; Okunloye, N. A.; Adesesan, A. A.; Edu-Muyideen, I. O.; Adedeji, A. M.; Ezechi, O. C.; Deji-Agboola, M. A. Occurrence and Clinical Characteristics of Vaginitis among Women of Reproductive Age in Lagos, Nigeria. *Adv. Reprod. Sci.* **2022**, *10* (4), 91–105.

(7) Itriyeva, K. Evaluation of vulvovaginitis in the adolescent patient. *Curr. Probl. Pediatr. adolesc. Health Care.* **2020**, *50* (7), No. 100836, DOI: 10.1016/j.cppeds.2020.100836.

(8) Palmeira-de-Oliveira, R.; Palmeira-de-Oliveira, A.; Martinez-de-Oliveira, J. New strategies for local treatment of vaginal infections. *Adv. Drug Delivery Rev.* **2015**, *92*, 105−122.

(9) de Cássia Orlandi Sardi, J.; Silva, D. R.; Anibal, P. C.; de Campos Baldin, J. J. C. M.; Ramalho, S. R.; Rosalen, P. L.; Macedo, M. L. R.; Hofling, J. F. Vulvovaginal candidiasis: epidemiology and risk factors, pathogenesis, resistance, and new therapeutic options. *Curr. Fungal Infect. Rep.* **2021**, *15*, 32−40.

(10) Bradshaw, C. S.; Sobel, J. D. Current treatment of bacterial vaginosis—limitations and need for innovation. *J. Infect. Dis.* **2016**, *214* (suppl_1), S14−S20, DOI: 10.1093/infdis/jiw159.

(11) Donders, G.; Sziller, I. O.; Paavonen, J.; Hay, P.; De Seta, F.; Bohbot, J. M.; Kotarski, J.; Vives, J. A.; Szabo, B.; Cepuliene, R.; Mendling, W. Management of recurrent vulvovaginal candidosis: Narrative review of the literature and European expert panel opinion. *Front. Cell. Infect. Microbiol.* **2022**, *12*, 1257 DOI: 10.3389/fcimb.2022.934353.

(12) Osmałek, T.; Froelich, A.; Jadach, B.; Tatarek, A.; Gadziński, P.; Falana, A.; Galińska, K.; Ekert, M.; Puri, V.; Wrotyńska-Barczyńska, J.; Michniak-Kohn, B. Recent advances in polymer-based vaginal drug delivery systems. *Pharmaceutics* **2021**, *13* (6), 884.

(13) Yang, J.; Liang, Z.; Lu, P.; Song, F.; Zhang, Z.; Zhou, T.; Li, J.; Zhang, J. Development of a Luliconazole Nanoemulsion as a Prospective Ophthalmic Delivery System for the Treatment of Fungal Keratitis: In Vitro and In Vivo Evaluation. *Pharmaceutics* **2022**, *14* (10), 2052.

(14) Koga, H.; Nanjoh, Y.; Makimura, K.; Tsuboi, R. In vitro antifungal activities of luliconazole, a new topical imidazole. *Med. Mycol.* **2009**, *47* (6), 640−647.

(15) Vanić, Ž.; Jøraholmen, M. W.; Škalko-Basnet, N. Nano-medicines for the topical treatment of vulvovaginal infections: Addressing the challenges of antimicrobial resistance. *Adv. Drug Delivery Rev.* **2021**, *178*, No. 113855, DOI: 10.1016/j.addr.2021.113855.

(16) Shetty, K.; Bhandari, A.; Yadav, K. S. Nanoparticles incorporated in nanofibers using electrospinning: A novel nano-in-nano delivery system. *J. Controlled Release* **2022**, *350*, 421−434, DOI: 10.1016/j.jconrel.2022.08.035.

(17) Singh, B.; Kim, K.; Park, M. H. On-demand drug delivery systems using nanofibers. *Nanomaterials* **2021**, *11* (12), 3411 DOI: 10.3390/nano11123411.

(18) Morie, A.; Garg, T.; Goyal, A. K.; Rath, G. Nanofibers as novel drug carrier−an overview. *Artif. Cells, Nanomed. Biotechnol.* **2016**, *44* (1), 135−143, DOI: 10.3109/21691401.2014.927879.

(19) Nenoff, P.; Haustein, U. F.; Brandt, W. Antifungal activity of the essential oil of Melaleuca alternifolia (tea tree oil) against pathogenic fungi in vitro. *Skin Pharmacol. Physiol.* **1996**, *9* (6), 388−394.

(20) Kumar, M.; Shanthi, N.; Mahato, A. K.; Soni, S.; Rajnikanth, P. S. Preparation of luliconazole nanocrystals loaded hydrogel for improvement of dissolution and antifungal activity. *Heliyon* **2019**, *5* (5), No. e01688, DOI: 10.1016/j.heliyon.2019.e01688.

(21) Hammer, K1; Carson, C. F.; Riley, T. V. Antifungal activity of the components of Melaleuca alternifolia (tea tree) oil. *J. Appl. Microbiol.* **2003**, *95* (4), 853−860, DOI: 10.1046/j.1365-2672.2003.02059.x.

(22) Kleijnen, J. P. C. Response surface methodology for constrained simulation optimization: An overview. *Simul. Modell. Pract. Theory* **2008**, *16* (1), 50−64, DOI: 10.1016/j.simpat.2007.10.001.

(23) Thakkar, S.; Misra, M. Electrospun polymeric nanofibers: New horizons in drug delivery. *Eur. J. Pharm. Sci.* **2017**, *107*, 148−167.

(24) Eichhorn, S. J.; Sampson, W. W. Relationships between specific surface area and pore size in electrospun polymer fibre networks. *J. R. Soc. Interface* **2010**, *7* (45), 641−649.

(25) Tiwari, K.; Bhattacharya, S. The ascension of nanosponges as a drug delivery carrier: Preparation, characterization, and applications. *J. Mater. Sci.: Mater. Med.* **2022**, *33* (3), 28.

(26) Patel, P.; Ahir, K.; Patel, V.; Manani, L.; Patel, C. Drug-Excipient compatibility studies: First step for dosage form development. *Pharma Innovation* **2015**, *4* (5), 14.

(27) Deepak, A.; Goyal, A. K.; Rath, G. Nanofiber in transmucosal drug delivery. *J. Drug Delivery Sci. Technol.* **2018**, *1* (43), 379−387, DOI: 10.1016/j.jddst.2017.11.008.

(28) Huang, F.; Wei, Q.; Cai, Y.; Wu, N. Surface structures and contact angles of electrospun poly (vinylidene fluoride) nanofiber membranes. *Int. J. Polym. Anal. Charact.* **2008**, *13* (4), 292−301.

(29) Ji, H.; Zhang, W.; Zhou, Y.; Zhang, M.; Zhu, J.; Song, Y.; Lü, J.; Zhu, J. A three-dimensional model of lanosterol 14α-demethylase of Candida albicans and its interaction with azole antifungals. *J. Med. Chem.* **2000**, *43* (13), 2493−2505, DOI: 10.1021/jm990589g.

(30) Gautam, S.; Dinda, A. K.; Mishra, N. C. Fabrication and characterization of PCL/gelatin composite nanofibrous scaffold for tissue engineering applications by electrospinning method. *Mater. Sci. Eng.: C* **2013**, *33* (3), 1228−1235, DOI: 10.1016/j.msec.2012.12.015.

(31) Tuğcu-Demiröz, F.; Saar, S.; Tort, S.; Acartürk, F. Electrospun metronidazole-loaded nanofibers for vaginal drug delivery. *Drug Dev. Ind. Pharm.* **2020**, *46* (6), 1015−1025.

(32) Kapileshwari, G. R.; Barve, A. R.; Kumar, L.; Bhide, P. J.; Joshi, M.; Shirodkar, R. K. Novel drug delivery system of luliconazole-Formulation and characterisation. *J. Drug Delivery Sci. Technol.* **2020**, *55*, No. 101302, DOI: 10.1016/j.jddst.2019.101302.

(33) Zhu, X.; Ni, S.; Xia, T.; Yao, Q.; Li, H.; Wang, B.; Wang, J.; Li, X.; Su, W. Anti-neoplastic cytotoxicity of SN-38-loaded PCL/Gelatin electrospun composite nanofiber scaffolds against human glioblastoma cells in vitro. *J. Pharm. Sci.* **2015**, *104* (12), 4345−4354.

(34) Tuğcu-Demiröz, F.; Saar, S.; Kara, A. A.; Yıldız, A.; Tunçel, E.; Acartürk, F. Development and characterization of chitosan nanoparticles loaded nanofiber hybrid system for vaginal controlled release of benzydamine. *Eur. J. Pharm. Sci.* **2021**, *161*, No. 105801.

(35) Subramanian, A.; Krishnan, U. M.; Sethuraman, S. Fabrication, characterization and in vitro evaluation of aligned PLGA−PCL nanofibers for neural regeneration. *Ann. Biomed. Eng.* **2012**, *40*, 2098−2110, DOI: 10.1007/s10439-012-0592-6.

(36) Sharma, R.; Garg, T.; Goyal, A. K.; Rath, G. Development, optimization and evaluation of polymeric electrospun nanofiber: a tool for local delivery of fluconazole for management of vaginal candidiasis. *Artif. Cells, Nanomed. Biotechnol.* **2016**, *44* (2), 524−531.

(37) Huang, Z. M.; Zhang, Y. Z.; Ramakrishna, S.; Lim, C. T. Electrospinning and mechanical characterization of gelatin nanofibers. *Polymer* **2004**, *45* (15), 5361−5368, DOI: 10.1016/j.polymer.2004.04.005.

(38) Szekalska, M.; Wróblewska, M.; Czajkowska-Kośnik, A.; Sosnowska, K.; Misiak, P.; Wilczewska, A. Z.; Winnicka, K. The Spray-Dried Alginate/Gelatin Microparticles with Luliconazole as Mucoadhesive Drug Delivery System. *Materials* **2023**, *16* (1), 403 DOI: 10.3390/ma16010403.

(39) Khan, G.; Yadav, S. K.; Patel, R. R.; Kumar, N.; Bansal, M.; Mishra, B. Tinidazole functionalized homogeneous electrospun chitosan/poly (ε-caprolactone) hybrid nanofiber membrane: Development, optimization and its clinical implications. *Int. J. Biol. Macromol.* **2017**, *103*, 1311−1326, DOI: 10.1016/j.ijbiomac.2017.05.161.

(40) Helal, D. A.; El-Rhman, D. A.; Abdel-Halim, S. A.; El-Nabarawi, M. A. Formulation and evaluation of fluconazole topical gel. *Int. J. Pharm. Pharm. Sci.* **2012**, *4* (5), 176−183.

(41) Singh, M.; Chauhan, D.; Das, A. K.; Iqbal, Z.; Solanki, P. R. PVA/PMMA polymer blended composite electrospun nanofibers mat and their potential use as an anti-biofilm product. *J. Appl. Polym. Sci.* **2021**, *138* (18), 50340.